OTC 19545

Comparison of Jackup Rig Spudcan Penetration Methods in Clay

David Menzies, Fugro-McClelland Marine Geosciences, Inc., and Richard Roper, ENSCO International, Inc.

This paper was prepared for presentation at the 2008 Offshore Technology Conference held in Houston, Texas, U.S.A., 5–8 May 2008.

Abstract

This paper compares four methods that predict jackup rig spudcan penetration with measured load-penetration records at thirteen Gulf of Mexico locations. Predicted load-penetration curves, for the four methods, are determined using site-specfic geotechnical information for normally to slightly over-consolidated clay soil profiles. The four methods include two based on SNAME (2002) recommendations, using bearing capacity formulations as proposed by Skempton (1951) and Hansen (1970), a method recommended by Houlsby & Martin (2003), and a method recommended by Hossain et al. (2006). Detailed spudcan geometries and dimensions from the seven different types of jackup rigs installed at the thirteen locations are also provided. Spudcan diameters of the seven jackup rigs vary from 11.0 to 20.1 meters and spudcan bearing pressures range from 162.8 to 507.4 kPa.

Interpreted soil parameters are presented for all thirteen sites. Boring logs, illustrating the interpretation of parameters from the measured soil properties are presented for two of these locations. The logs present the results of standard laboratory tests typically performed for Gulf of Mexico site investigations: undisturbed undrained shear strength measurements from Torvane, miniature vane, pocket penetrometer and unconsolidated-undrained (UU) triaxial tests; remolded shear strength from miniature vane and UU triaxial tests; submerged unit weights (derived from measured bulk wet unit weight); water content; and Atterberg limits. Theoretical submerged unit weight values, used as an aid in parameter selection, are also plotted on the boring logs.

The results of this study are presented in a series of figures that compare the predicted load-penetration curves based on each of the four methods to the measured load-penetration data recorded during the installation of the jackup rig at each of the thirteen locations. The comparisons indicate that (1) the Houlsby & Martin method provides good lower bound load-penetration predictions, generally predicting a deeper penetration under a given load than measured; (2) the Hossain et al., method provides an upper bound load-penetration prediction, usually predicting a shallower penetration under a given load than that measured, and (3) the modified SNAME methods, with Skempton and Hansen bearing capacity factors, provide reasonable predictions of the average penetration under a given load.

Two factors affecting the predictions are also discussed: spudcan geometry and spudcan cavity depth. The results demonstrate the difficulties all four methods may experience providing accurate load-penetration predictions for jackup rigs with spudcan geometries that do not lend themselves to easy modeling using standard bearing capacity factors and equivalent projected circular bearing areas. At four of the sites, with three different types of jackup rigs, all of the four methods provide more acceptable predictions after application of empirical rig-specific correction factors. The depths of spudcan cavities are examined using the methods presented in SNAME (2002) and recommendations in the Hossain et al. (2006) paper. The effects of spudcan cavity depth on the load-penetration behavior during preload and on the ultimate bearing capacity are discussed in this paper.

Introduction

Ten independent leg jackup rigs in the Gulf of Mexico either sustained severe damage or were completely lost during severe storms of the 2004 and 2005 hurricane seasons (Jack et al., 2007). These losses have been attributed to larger than anticipated storm waves, in some cases placing the jackup rig hulls within the wave zone, and ultimately overloading the foundation and/or structural components of the legs (Morandi, 2007).

The losses have prompted actions, to reduce the chances of future losses, and research to better understand and predict foundation behavior of independent leg jackup rigs. API RP 95J (2006) and the U.S. government Mineral Management Service (MMS) highly recommend that site-specific spudcan penetration assessments be performed and larger jackup rig hull-to-mean-sea-level air gaps be used during hurricane season. A comprehensive joint industry study of jackup rig spudcan behavior, designated the InSafeJIP™, has been implemented by the international community with recommendations expected as early as March of 2009. The International Association of Drilling Contractors (IADC) has also funded a study to compare bearing capacity methods and provided the funds for the analysis of a majority of the data presented in this paper.

New and revised bearing capacity methods to predict spudcan penetration for normally consolidated clay sites are presented in SNAME (2002), Houlsby & Martin (2003) and Hossain et al. (2006). These methods predict somewhat different load-penetration responses. To evaluate the ability of these methods to accurately predict the load-penetration response of jackup rig spudcans, predictions are compared to measured load-penetration records obtained during preloading of jackup rigs at thirteen different locations in the Gulf of Mexico where the soils were predominately normally to slightly over-consolidated clay. The specific locations chosen all had (1) good site-specific soil information, (2) accurate spudcan penetration records, and (3) jackup rigs with well-documented spudcan geometries. Unfortunately, this information is not always available, and, when it is, it is seldom from a single source. This information may be assembled by; polling the operators (oil companies), geotechnical consultants, drilling contractors, rig designers and marine warranty surveyors. Site-specific soil data was not required in the past and still is not required except when the rigs are to be in operation during hurricane season. Data from nine of the thirteen sites include detailed load-penetration records, with intermediate load-penetration values recorded between the "initial" penetration values, immediately after the hull was jacked from the water, to the "final" penetration values after all stages of preload ballasting were completed. These detailed records are difficult to find since many drilling contractors only record initial and final spudcan penetration values. Further complicating detailed comparison of the predictive methods is the fact that jackup rig spudcan drawings, providing detailed spudcan shapes and dimensions, are not readily available. Drawings obtained from literature or drilling contractors may differ from actual builder specifications, while obtaining drawings from rig designers and builders is difficult as spudcan designs are proprietary. Even with detailed spudcan drawings from rig designers, the areas and volumes determined from these drawings often vary depending on the level of detail used to analyze and determine these values due to their complicated shapes.

Soil Conditions and Parameter Selection

Gulf of Mexico soil investigations typically consist of one soil boring with laboratory testing performed on soil samples recovered using open-hole rotary drilling techniques. Historically, most soil borings performed on the Gulf of Mexico shelf were performed to provide pile design data. However, recent requests to perform soil investigations for jackup rig spudcan analysis have increased in the past few years due to API RP 95J requirements. If a site investigation includes a request for spudcan penetration analysis, the sampling program for pile design data is modified to include additional samples at 1.5 m spacing, typically in the 12 to 30 meter penetration range to increase the density of test data presented on the boring log. Occasionally, in situ testing (cone penetrometer testing or in situ vane) and / or soil borings are performed at multiple locations if spatial soil variability is suspected. However, this is typically not the norm for jackup rig soil investigations in the Gulf of Mexico. At each of the sites used in this study, only a single boring was drilled and sampled. The soil borings were usually located near the stern leg position of the jackup rigs; however, the exact distances from the borings to the spudcan positions were not determined.

The selection of appropriate soil parameters has the greatest impact on how accurate an estimate of spudcan load-penetration will be derived using any of the proposed methods. The selection of soil parameters is somewhat subjective and relies upon local geotechnical experience (Quiros et al., 2008). During the selection process, it is important to understand the limitations of sampling and testing procedures, and to be familiar with the methods used to interpret test results based on the specific soils (in this case, soft to stiff, normally to slightly over-consolidated Gulf of Mexico clay), and to understand the design methods to be employed. To reduce subjectivity in the selection of parameters needed for bearing capacity analysis, more soil information than is usually obtained would be required. This information could be provided with (1) multiple soil borings, one at each spudcan location, (2) in-situ testing, and (3) advanced laboratory soil tests that identify and reduce the effects of sample disturbance. Soil parameters selected for the thirteen sites in this paper are presented in Table 1.

Soil parameters presented in Table 1 were selected using methods commonly employed in normally consolidated clays to penetrations of concern in rig penetration studies. Straight trend lines were fit through the soil test data that best capture the interpreted in-situ shear strength and submerged unit weight profiles. The positioning of these trend lines relative to the "undisturbed" test data is based on the author's experience with these types of soils and their in-situ response during spudcan penetration. Measured values of undrained shear strength and submerged unit weight may be artificially low due to soil disturbance. Reviewing the soil sensitivity, water content, liquidity index and plasticity index can often identify where this occurs.

Theoretical submerged unit weight values, although not measured data, are plotted on the boring logs to assess in-situ submerged unit weight values and identify zones of possible soil disturbance. Theoretical unit weight values, measured in units of kN/m^3, are determined using the following expression.

$$\gamma'_{th} = 9.80 \left[\frac{Gs(1+0.01w)}{1+0.01wGs} \right] - 10.05 \qquad (1)$$

The terms used in the above expression are defined in the nomenclature section. Differences between theoretical and measured submerged unit values are often attributable to sample disturbance caused by stress relief and sample expansion.

Measures of soil sensitivity, the ratio of undisturbed to remold shear strength, were also helpful in the identification of acceptable shear strength test data. Soil sensitivity values that range from 2 to 3.5 are typical of the values measured for the sites in this study.

Local experience in the selection of soil parameters at the thirteen sites included consideration of soil conditions at nearby investigation sites and historical spudcan penetration records. The use of such additional information is particularly beneficial when analyzing soil data obtained in the 1960's and 1970's, consisting of test results performed on small diameter driven samples, or when the soils are highly expansive and gassy, a condition that increases sampling disturbance. Shear strength test data at older investigation sites are often low and must be adjusted (Quiros et al., 1983) to assess the in-situ shear strength appropriate for bearing capacity predictions and spudcan penetration estimates.

Soil information for Sites 3 and 10 are shown graphically in Figure 1 in the form of logs of boring and test results, or as more commonly known, "boring logs". These two boring logs are typical of the soil conditions at the other 11 locations used for this study. Site 3 soil conditions consist of a very soft to stiff normally consolidated clay with linear shear strength and unit weight profiles that increase with penetration. Soil conditions for Site 10 consist of slightly over-consolidated soft to stiff clay. The soil parameter trend lines for undrained shear strength and submerged unit weight for both sites are shown on the boring logs in Figure 1.

The undrained shear strength profiles for all but two of the thirteen sites could be adequately represented using a trend line that increased linearly from the mudline to well below the depth of interest. Sites 6 and 10, however, have a two-layer soil stratigraphy consisting of a normally consolidated soft clay drape underlain by older, slightly over-consolidated clay. To apply the bearing capacity methods of Houlsby & Martin and Hossain et al., the shear strength profile of the deeper layer was projected to the mudline and the profile in the shallow drape clay ignored. (This method should not significantly affect the results as the first measured penetration values, the initial spudcan penetrations, were below the base of the drape sediment layer).

Jackup Rig Loads and Spudcan Geometries

Seven different types of independent leg jackup rigs, with different tank-type spudcan shapes and maximum bearing pressures, were selected for this study. For each of the seven different jackup rig types, the spudcan equivalent diameter, maximum cross sectional area, volume, and maximum bearing pressures are presented in Table 2. Six of the jackup rigs in this study are Marathon LeTourneau designs and one is a Levingston design. The spudcan maximum cross sectional areas range from 87.7 to 306.7 square meters and maximum bearing pressures vary from 162.8 to 507.4 kPa. This broad range in spudcan dimensions and bearing pressures was selected to provide a rigorous test of the four bearing capacity methods evaluated in this study.

The shapes and dimensions of the spudcans used in this study are shown in Figure 2. Plan views display the maximum cross sectional areas (maximum projected areas). Profile views detail the projection of the spudcan tips beneath the widest cross section, and give a general indication of the volumes of soil displaced beneath the major cross-sectional area. The spudcans shown in Figure 2 are drawn to scale to allow easy comparison of the different sizes and tip lengths. The spudcan cross-sectional shapes are either circular, truncated circular, hexagonal, or dodecagonal. In this study, all were analyzed as circular shapes with diameters selected to yield cross-sectional areas equivalent to the actual spudcans maximum cross-sectional areas.

As jackup rigs increase their leg load, either to raise the hull above the water or during preload operations, the spudcan penetrates into the soil until the soil bearing capacity meets or exceeds the applied load. As the spudcan penetrates, the soil below the spudcan fails, and the soil is displaced. This soil is pushed outward from beneath the spudcan and may flow onto the top of the spudcan, depending on the depth of embedment (Hossain el al. 2006). The length of the spudcan tip is, generally, related to the volume of the spudcan below the major cross-sectional area. A spudcan with a large tip length will usually have a larger volume below the major cross-sectional area and displace more soil from beneath the spudcan, whereas a relatively flat spudcan with little or no spudcan tip will fail the soil nearer the major cross section. Thus, it appears that spudcan shape influences bearing capacity efficiency.

When spudcans penetrate into soil, a cavity may develop between the top of the spudcan and the mudline. Many researchers, mostly through the use of centrifuge testing, are currently studying the stability of this cavity and its tendency to backflow and fill. However, many of these centrifuge tests do not account for the leg trusses that extend from the tops of the spudcans to the jackup rig hull. These leg truss members may provide support for the soil above the top of the spudcans and slow the cavity backfill process. The implications of a slowed backfilling are discussed later.

Spudcan Penetration Records

Jackup rig spudcan penetration depths are determined from marking on the leg and subtracting the leg guide housing height, height of the rig hull, air gap, and water depth (Young et al., 1984). Spudcan tip lengths range from 2.3 to 3.5 meters for the jackup rigs in this study. The majority of the penetration records in this paper were provided by ENSCO International, Inc. These records consist of load and spudcan tip penetration values measured at closely spaced load-penetration intervals for the three legs during preload operations. GlobalSantaFe Corporation (now Transocean, Inc.), Rowan Companies, Inc., and Diamond Offshore Drilling, Inc., also provided spudcan penetration records for this study. Less detailed penetration records that consist only of initial and final load-penetration values, often with only one value presented for all three legs are common. The spudcan penetration records for Sites 6, 10, 11 and 13 in this study consist of only initial and final penetration values.

During preload operations with rigs located in normally consolidated clay soil profiles, spudcans often penetrate as much as an additional 6 to 20 meters over their initial penetration. This additional penetration occurs during a series of preload sequences or “stages” where the jackup rig hull is positioned about 1.5 m above average sea level, the ballast load is slowly increased, the spudcans penetrate into the soil and the jackup rig hull approaches sea level. Once the jackup rig hull comes into contact with the water, preloading is stopped, the ballast water is dumped, and the jackup rig hull is elevated another 1.5 meter above sea level. These preload stages are repeated until the maximum preload value is obtained, held for a designated time, and no additional spudcan penetration occurs. Idealized and measured spudcan penetration records, for a typical normally consolidated clay location, are shown in Figure 3.

Figure 3 reveals that the measured load-penetration values are not as smooth, linear and continuous as idealized. The measured values are complicated by operational issues and may be further complicated by the fact that each leg may have been loaded individually. Before comparing these records to predicted load-penetration curves, the data were edited to include only steps where an increase in load was accompanied by an increase in penetration.

In spite of this care, actual spudcan load-penetration records are somewhat imprecise. Where the load-penetration records appear unusual, reasons why should be explored. Some of the reasons for scatter in the measured load-penetration data include the following possibilities:

1. Preloading the leg individually may result in different penetration rates and variations in the datum used to determine penetration depths,
2. Soil setup, a strengthening of the soil beneath the spudcans, may have occurred from delays between preload stages,
3. Spudcans may be in close proximity of existing (old) spudcan depressions and pockmarks,
4. Thin granular layers or other anomalous soil conditions (from soil variability) may influence soil properties,
5. Errors in the measured penetration values may occur from changing tidal conditions, human error, or eccentricity from P-Δ (leaning instability) effects,
6. Load values may be inaccurate due to hull buoyancy, once the jackup rig hull drops into the wave zone,
7. Waves hitting the hull may add dynamic and cyclic effects to the loading process,
8. Penetration values may not have been recorded at close enough depth intervals to indicate the spudcan penetration path, and
9. Backfill of soil on top of spudcans may vary depending on soil type, spudcan geometry, and influence from the leg trusses.

Bearing Capacity Methods

This paper compares four methods that predict jackup rig spudcan penetration. The four methods include two based on SNAME (2002) recommendations, using bearing capacity formulations as proposed by Skempton (1951) and Hansen (1970), a method recommended by Houlsby & Martin (2003), and a method recommended by Hossain et al. (2006). Results of computed spudcan penetration are compared with measured spudcan load-penetration records.

Inputs for these methods are soil parameters, including shear strength and submerged unit weight profiles, and spudcan properties, including the maximum cross-sectional area, volume of displaced soil, and spudcan tip angle. The more recent methods by Houlsby & Martin and Hossain et al., are recommended for application at sites where the soil shear profile increase linearly with increasing depth. Sites with these types of soil conditions were, therefore, selected specifically for this study.

Jackup rig spudcan foundations apply bearing pressures to the soil and continue to penetrate until the bearing capacity of the soil is equal to or exceeds the applied spudcan pressure. For normally consolidated clay sites, spudcan penetration will occur continuously as additional preload is added and transferred through the leg trusses to the spudcans. Different methods exist to predict spudcan penetration and all are highly dependent upon using the correct shear strength. The four bearing capacity methods that are compared with measured spudcan penetration records are discussed below.

Skempton Method. Gemenhardt & Focht (1970) and later Young et al. (1984) discuss the use of Skempton’s bearing capacity, shape, and depth factors to determine spudcan penetration. Similar factors are also recommended by SNAME (2002) and ISO (2003). A basic equation to determine load, using factors recommended by Skempton, for spudcan penetration assessment with no soil backflow follows:

$$Q = \left[5.14 * (1 + 0.2\frac{B}{L})(1 + 0.2\frac{D}{B}) s_{uavg} + \gamma_H{}' H\right] A + \gamma' V \qquad (2)$$

Many of the above terms are indicated in Figure 4 and all the terms are listed in the nomenclature section of this paper. The above equation can be simplified if the B and L terms are assumed to be equal (e.g., an equivalent circular spudcan shape) and the $\gamma_H{}'H$ term becomes zero if the soil above the spudcan is assumed to backflow and completely fill the spudcan cavity. Complete soil backflow into the spudcan cavity is a reasonable assumption in normally consolidated clay soils. With these simplifications, Equation 2 reduces to:

$$Q = \left[6*(1+0.2\frac{D}{B})s_{uavg}\quad\right]A + \gamma' V \qquad (3)$$

The terms required to compute the bearing capacity of the soil beneath the spudcan using the Skempton Method and Equation 3 are: (1) D, the depth of the spudcan maximum cross sectional area below the mudline; (2) B, the equivalent spudcan diameter; (3) s_{uavg}, average shear strength below the major cross section of the spudcan; (4) A, the major cross sectional area of the spudcan; (5) γ', average submerged unit weight of soil displaced by the spudcan; and (6) V, the volume of the spudcan. In this study, s_{uavg} was computed as the average shear strength to a depth of one-half the spudcan diameter below the spudcan major cross section (therefore, 5.3 to 9.9 meters below the major cross section in this study), as recommended by Young et al. (1984).

The depth factor 1+0.2(D/B) is limited to values less than or equal to 1.5 (or D/B ≤ 2.5) in Equations 2 and 3 and the equations should be used only where shear strength profiles increase gradually with depth.

In normally consolidated clay profiles, the bearing capacity value computed for a given spudcan tip penetration is equivalent to the predicted spudcan load that will result in the spudcan penetrating to that same depth. For comparison to recorded load-penetration data, the computed bearing capacity (spudcan load) values are plotted at a depth (D) plus the length of the spudcan tip.

Hansen Method. Hansen (1970) recommended a bearing capacity method that has been adopted by Fugro-McClelland Marine Geosciences, Inc., (FMMG) to compute load-penetration values for jackup rig spudcan foundations. This method is similar to the expression presented above but uses the Hansen bearing capacity factor and a lower average shear strength value. The general expression, using the Hansen bearing capacity factor, to compute spudcan penetration with no soil backflow is as follows:

$$Q = \left[5.14*(1+0.2\frac{B}{L}+0.4\tan^{-1}\frac{D}{B})s_{uavg} + \gamma_H' H\right]A + \gamma' V \qquad (4)$$

The terms in this equation have been presented previously and are explained in the nomenclature section of this paper. This equation can be simplified for spudcan shapes that are approximated as circular and assuming complete backfill of the spudcan cavity. Making these assumptions the Equation 4 reduces to:

$$Q = \left[5.14*(1.2+0.4\tan^{-1}\frac{D}{B})s_{uavg}\quad\right]A + \gamma' V \qquad (5)$$

Experience has shown that calculating the average shear strength within the soil from the depth of the maximum cross section to a depth one-fourth of the equivalent spudcan diameter below works well with this method. The Hansen Method has no depth limitation and requires that soil properties be investigated to at least the depth of the spudcan tip (usually about B/4 below the maximum cross section). This depth range recommended for use in deriving the average shear strength approximates the depth of soil failure seen in centrifuge tests (Hossain et al., 2006).

Houlsby & Martin Method. A recent paper by Houlsby and Martin (2003) presents an analysis of the bearing capacity, which incorporates the spudcan tip design features, such as the "cone" angle, cone roughness, and depth of embedment as well as the rate of shear strength increase with depth. The method was developed for sites with clay shear strength profiles that increase linearly with increasing depth. A general expression to determine the load the spudcan can support, using the bearing capacity recommended by Houlsby and Martin, with no soil backflow, is as follows:

$$Q = \left[\; N_{co}s_{uo} + \gamma_H' H \;\right]A + \gamma' V \qquad (6)$$

The terms in the above expression have been introduced previously and are presented in the nomenclature section of this paper. The above expression can be simplified if the soil is assumed to completely backflow and fill the spudcan cavity as follows:

$$Q = N_{co}s_{uo}A + \gamma' V \qquad (7)$$

The bearing capacity factor, N_{co}, for linearly increasing shear strength profiles with increasing depth and for smooth footings can be derived using the following equations:

$$N_{co} = N_{co\alpha} + \frac{\alpha}{\tan(\frac{\beta}{2})}\left[1 + \frac{1}{6\tan(\frac{\beta}{2})}\frac{B\rho}{S_{uo}}\right] \quad (8a)$$

$$N_{co\alpha} = N_{coo}\left[1 + (0.212\alpha - 0.097\alpha^2)(1 - 0.53\frac{D}{B+D})\right] \quad (8b)$$

$$N_{coo} = N_1 + N_2\frac{B\rho}{S_{uo}} \quad (8c)$$

$$N_1 = 5.69\left[1 - 0.21\cos(\frac{\beta}{2})\right](1 + \frac{D}{B})^{0.34} \quad (8d)$$

$$N_2 = 0.5 + 0.36\left[\frac{1}{\tan(\frac{\beta}{2})}\right]^{1.5} - 0.4(\frac{D}{B})^2 \quad (8e)$$

For the above equations, the new terms are as follows: (1) s_{uo}, is the shear strength at the depth of the spudcan maximum cross-sectional area; (2) α, is a roughness term for the spudcan equal to 1.0 (rough footings) for this study; (3) β, is the angle of the spudcan cone; and (4) ρ, is the rate of shear strength increase with depth. The other terms were introduced previously, can be found in the nomenclature section or are indicated in Figure 4. The cone angle of spudcans is shown in Figure 2. Where more than one cone angle is shown for a given spudcan on Figure 2, the largest cone angle, the angle coincident with the majority of the spudcan tip volume was used for this study.

Hossain et al., Method. Hossain et al. (2006) present an analysis of spudcan penetration behavior based on centrifuge testing and finite element modeling. The paper investigates the soil flow mechanisms around the spudcan, the extent of the spudcan cavity, and spudcan penetration resistance. The method was developed for clay soil sites with shear strengths linearly increasing with increasing depth below the mudline. The equation to determine the capacity of the soil at shallow depth with an open cavity, using the bearing capacity factor (N_{co}) recommended by Hossain et al., is as follows:

$$Q = (N_{co}s_{uo} + \gamma_H' H_{cr})A + \gamma' V \quad (9)$$

The above equation can be simplified if the soil cavity above the spudcan is assumed to completely backfill or if the depth of spudcan embedment exceeds the critical depth of the soil cavity, and the cavity remains unchanged and stable, as follows:

$$Q = N_{cd}s_{uo}A + \gamma' V \quad (10)$$

The above bearing capacity factor is expressed as follows:

$$N_{cd} = 10(1 + 0.075\frac{D}{B}) \qquad \text{For } \frac{H}{B} < \frac{D}{B} \leq 2 \text{ and} \quad (11a)$$

$$N_{cd} = 11.5 \quad \text{For } \frac{D}{B} > 2 \quad (11b)$$

Equation 9 was used to determine bearing capacity at sites where shallow penetration, less than the critical depth of the spudcan cavity, occurs. An expression for the bearing capacity term N_{co} is not provided in the Hossain et al., paper but tabulated values were provided and used to calculate load values for spudcans at shallow penetrations. The above bearing capacity term is expressed in terms of dimensionless depth ratio and soil strength non-homogeneity factors for rough spudcans. Equation 9 was used to determine the load at shallow penetration depths for Sites 4, 9, 11, 12, and 13 in this study. To extend the Hossain et al., predicted load-penetration curves to depth, a short transition zone must be handled between

Equation 9 and Equation 10, when the spudcan penetration depths are between the critical cavity depth, H, and not yet deep enough that the cavity is stabilized. We used interpolation between these depths to estimate spudcan loads.

Spudcan Cavity Depth

The behavior of the soil above the spudcan can influence the bearing pressure applied to the soil below, thus reducing penetrations if the cavity remains open or increasing penetrations if the cavity backfills. If the spudcan cavity collapses and backfill occurs after preloading has been completed, additional penetration or a reduction in the maximum top-side loads the rig can withstand before foundation (bearing capacity) failure occurs. Such a loss in load carrying capability reduces the available factor of safety and may place the jackup rig at higher risk of sustaining damage or loss in severe storms. Expressions to evaluate the spudcan cavity are presented below.

The SNAME (2002) document recommends the following method be used to determine the depth of the spudcan cavity.

$$H_{cr} \leq \frac{N s_{uH}}{\gamma_o'} \qquad (12)$$

The above expression uses the Meyerhof (1972) stability factor, N, to provide a conservative estimate of spudcan cavity depth. The remaining terms have been discussed previously, are indicated in Figure 4 and in the nomenclature section of this paper. The cavity depths determined for the thirteen locations in this study using the Meyerhof stability factors are presented in Table 3. The soil parameters presented in Table 1 were used to find the soil cavity heights. Reviewing the Meyerhof critical depths on Table 3, spudcan cavity depths of 5.8 to 23.6 meter were calculated. At seven of the thirteen sites, calculated spudcan cavity depths extend to the final spudcan penetration depth. For the normally to slightly over-consolidated clay sites such as selected for this study, these depths seem unlikely. SNAME (2002) also suggests that a stability factor recommended by Britto & Kusakabe (1983) could be used to determine the cavity depths at sites consisting of normally consolidated clay. The Britto & Kusakabe method was examined, but also resulted in spudcan cavity depths that seem unreasonably deep.

A method recommended by Hossain et al., (2006) was also used to determine spudcan cavity depths for sites in this study. They recommend the following expression:

$$\frac{H_{cr}}{B} = \left[\frac{S_{um}}{\gamma'_H B}\right]^{0.55} - \frac{S_{uH}}{4\gamma'_H B} \qquad (13)$$

The above expression is solved by iteration, selecting a depth H_{cr}, and determining the soil parameters for that depth. The submerged unit weight term is not very sensitive to change so an average value can be used. The depths of the spudcan cavity calculated for the thirteen sites using the above expression are also shown in Table 3. Hossain et al., spudcan cavity depths varied from 3.4 to 7.9 meters. These spudcan cavity depths were used to determine load-penetration values at sites with shallow penetration records. The cavity depths determined from the Hossain et al., expression seem reasonable and better fit the assumptions used to determine bearing capacity in this study. Additionally, Hossain et al., discuss that the spudcan cavity depth should remain unchanged once the critical or equilibrium depth is obtained. This assumption is examined when spudcan penetration records are reviewed later in this paper.

The above methods were derived from the stability of open excavations (Meyerhof) or from modeling of spudcan penetration during centrifuge testing and finite element modeling (Hossain et al.) The Meyerhof method is limited in that it does not consider the forces generated from soil displaced from beneath the spudcan. The method recommended by Hossain et al., gives reasonable values based on centrifuge model testing. However, the Hossain et al., method does not appear to account for the influence of the spudcan leg trusses, which may temporarily inhibit soil from backfilling inside the leg trusses.

In an attempt to better understand the behavior of the spudcan cavity, the detailed load-penetration records available at nine of the thirteen sites (Sites 1, 2, 3, 4, 5, 7, 8, 9, and 12 of Figure 5) were examined. Soil backflow was estimated at these sites by observing where changes in the slope of measured spudcan penetration records occur. Where the load-penetration response becomes steeper than that estimated based on the increase in theoretical bearing capacity (which is nearly linear with depth in normally consolidated clay profiles), soil backflow is thought to have occurred, thus applying additional, unrecorded spudcan loads. The records where there is no indication of additional penetration from soil backflow are described as “stable” in Table 3. A review of the Table 3 “observed cavity behavior” column indicates that seven of the nine detailed spudcan penetration records have unstable spudcan cavities where soil backfill is occurring during preload operations. The implications of these soil backflow observations are discussed in more detail in the section below.

Comparison of Results

Theoretical spudcan load-penetration curves were prepared using bearing capacity factors recommended by Skempton (1951), Hansen (1970), Houlsby & Martin (2003), and Hossain et al. (2006) and compared to measured spudcan load-penetration records. Theoretical and measured spudcan load-penetration curves are presented in Figure 5 for thirteen Gulf of Mexico locations. Seven different types of jackup rigs were analyzed with bearing pressures that varied from 162.8 to 507.4 kPa. The curves in Figure 5 are presented as load per individual spudcan (spudcan load) versus spudcan tip penetration, a penetration figure commonly used in the field records (spudcan tip lengths are detailed in Figure 2). Theoretical spudcan loads were determined using (1) the soil properties listed in Table 1, (2) the four bearing capacity methods mentioned previously, and (3) jackup rig spudcan properties and dimensions detailed in Table 2 and Figure 2, respectively. The following are observations made from the comparison of predicted and measured load-penetration curves presented in Figure 5. These observations will be discussed in terms of predicted versus observed penetrations.

The Houlsby and Martin method provides a good lower bound estimate of spudcan penetration for most sites, normally predicting slightly deeper penetrations under a given load than the observed values. Penetrations predicted using the Skempton and Hansen methods provide a good average estimate ("best estimate") of penetration for most sites, sometimes under-estimating penetration (e.g., the bow leg at Site 1) and sometimes over-estimating penetration (e.g., the bow leg at Site 2). The method recommended by Hossain et al., provides an upper bound estimate of spudcan penetration, usually predicting shallower penetrations under a given load than observed. However, if the estimated bearing capacity of the soil derived from the Hossain et al., method is reduced by 20 percent, predicted penetrations similar to the "best estimate" Skempton and Hansen values are obtained.

The predicted penetration curves for Sites 6, 10, 12, and 13 would not fit the measured records using the standard parameters. Empirical adjustment factors, ranging from 0.85 to 0.9 were applied to the theoretically derived bearing capacities to obtain acceptable predicted load-penetration curves in line with their relationships to the observed load-penetration records. The explanation for the required empirical adjustment factors is discussed in more detail in comments specific to these locations that appear below.

Ten of the thirteen load-penetration records shown in Figure 5 include penetrations values for all three of the rig's spudcans (bow, starboard and port). A review of the penetration records for these ten sites reveals a range in penetration values under a given spudcan load for many of the sites. Reasons for this scatter in the measured records were discussed previously and may be related to (1) preload and measurement procedures, (2) interpretation of the records, (3) variations in soil conditions, (4) influence from old spudcan depressions, and (5) changing and unaccounted for loads due to spudcan cavity instability. Such scatter in observed penetration records is typical. Consequently, in practice a range of predicted load-penetration curves bounding the expected behavior is appropriate and usually provided to drilling contractors to capture the expected range of the load-penetration responses typically encountered at Gulf of Mexico sites.

Site-specific comments comparing the predicted and observed load-penetration curves shown in Figure 5 are presented below.

Site 1. Both the Hossain et al., and Skempton predicted load-penetration curves predict a linear response below 30 and 36.5 meters, respectively, in accordance with their derivation of bearing capacity factors. However, the observed penetrations extend to 41 meters below mudline. An examination of the measured penetration records at the end of preload operations indicates additional spudcan penetration, another 1 to 2 meters, occurs at a near constant load for all three legs. As discussed previously, a likely cause for this additional penetration is soil backflow into the spudcan cavity. The predicted spudcan penetrations based on the Skempton method under-predict measured penetration values by as much as 4 meters. At deep-water sites, such a large discrepancy between predicted and actual penetrations could result in a jackup rig mobilizing to a location only to discover it has insufficient leg length to work.

Site 2. Measured port leg penetration records that fall below the Houlsby & Martin curve are probably related to problems with interpreting the penetration records during pre-load stages or due to eccentric loading (tilting of the rig while ballasting). These low measured values should probably be ignored; however, they demonstrate the problems inherent in interpreting the measured penetration records. Reasons for low bow penetrations could also be related to load eccentricity, soil variability or spudcan cavity behavior. The spudcan cavity appears stable since there is no indication of additional penetration after achieving maximum preload values.

Sites 3, 4, 5 & 11. Predicted spudcan penetration values for Site 3 follow the measured load-penetration curves. Relatively higher measured bow penetration values between 24 and 27 meters may be related to soil variability. The spudcan cavity appears to be stable for Site 3. Site 4 penetration records display more significant scatter. The scatter in these records is likely related to staged loading and interpretation of records. Below 12 to 15 meter penetration at Site 4, additional observed spudcan penetration occurs while maximum (full preload) spudcan loads remain constant. This additional penetration may be attributable to increased and unaccounted for loading from soil backfill. Predicted penetration curves generally follow the measured penetrations at Site 5, but additional penetration occurs below 17 to 18 meter penetration while holding maximum preload. Once again, additional spudcan penetration is probably related to increased and unaccounted for load from the backflow of soil into the spudcan cavity. Only the initial and final spudcan penetrations were recorded at Site 11. Predicated and measured values correlate well. Data from Site 11 was included to provide a relatively small spudcan size, that of the Marathon LeTourneau 150-44-C type jackup rig.

Sites 6 & 10. Predicted spudcan penetration curves for Sites 6 and 10 were adjusted by empirical factors of 0.85 to better match the measured spudcan penetration records for the Super Gorilla jackup rig, the heaviest loaded jackup rig in this study. This empirical adjustment factor has been applied in practice at other sites where this jackup rig has worked. The need for an adjustment factor may be related to the shape and volume of the spudcan. Dimensions for the spudcan of the Super Gorilla are shown in Figure 2. An examination of the Super Gorilla spudcan shape indicates that it is asymmetrical, featuring a short dimension from the center of the spudcan to the outer edge of 9 m and a long dimension of 10.1 m. As discussed previously, an equivalent spudcan diameter, 19.8 m, assuming a circular shape and derived based on the maximum cross-sectional area, was used for this study. If the effective area of the spudcan is reduced to only encompass the shortest dimension, an equivalent diameter of 18 meters, the effective bearing area of spudcan will be reduced to 83 percent of the valued used for this study. Additionally, the Super Gorilla spudcan tip (cone) extends 2.8 m below the maximum cross-sectional area. When compared to other spudcan tip lengths in Figure 2, the Super Gorilla spudcan tip appears short relative to the spudcan diameter. Consequently, the Super Gorilla spudcans will not displace the same amount of soil beneath its widest section in proportion to the other Marathon LeTourneau jackup rigs in this study. These dimensional aspects of the Super Gorilla spudcans may explain the need for application of the empirical "shape factor" to the theoretical load-penetration curves in order to obtain reasonable penetration predictions.

Sites 7, 8 & 9. The predicted trends closely follow the measured penetration records at Site 7 to 23 meters penetration. Below 23 meters penetration, additional loading from soil backflow into the spudcan cavity appears to have occurred. Similarly, at Site 8, measured penetration records suggest soil backflow into the spudcan cavity beginning below about 22 meters penetration. The cavity appears to backflow at different depths, or at least at different rates for the port and bow legs, although these differences could also be related to differences in soil lateral variability. Predicted penetrations generally underestimate observed penetrations above 8.5 meters for Site 9. This may be an indication of soil disturbance from previous spudcan installations. Often the site-investigation data at Gulf of Mexico sites has been obtained prior to earlier jackup rig installations and the associated soil disturbance is not captured in the soil strength profiles. Below 8.5 meters penetration, the predicted load-penetration curves correlate well with the measured data, suggesting that the spudcan bearing pressures of the rig analyzed are higher than the earlier rig, and the spudcans have penetrated into undisturbed soils. Below 10 meters penetration, a small amount of additional penetration from soil backflow appears to occur.

Sites 12 & 13. The jackup rigs positioned at Sites 12 and 13 were the Levingston, Class 111-IC and Marathon LeTourneau, Class 52-S, respectively. The configuration of the spudcans for these jackup rigs is shown in Figure 2. An examination of these drawings indicates that the spudcans have relative large spudcan bearing areas with relatively short spudcan tip (cone) lengths, which reduces the proportion of soil displaced relative to the penetration of the maximum cross-sectional area. In addition, the profile of the Class 52-S spudcan tip is concave, further reducing the amount of soil the spudcan tip displaces. In order for the theoretical load-penetration curves to present reasonable predictions of the measured penetration records, the theoretical curves for Sites 12 and 13 required an empirical "shape factor" modification of 0.9, a factor commonly applied in practice for these two types of rigs. The penetration records for Site 12 show additional penetration after establishing maximum preload, suggesting spudcan cavity instability and soil backflow. Both of these jackup rigs have relatively low bearing pressures.

Spudcan Cavity Instability and Soil Backflow

At sites where deep spudcan penetrations are expected, typical of those presented in this study, it is possible that the structural trusses and cords of the jackup legs provide some temporary resistance to soil backflow into the spudcan cavity. This would explain the observed additional penetrations that occur under the constant rig preload pressures in many of the spudcan penetration records selected for this study. Spudcan cavity instability and soil backflow after completion of the preloading operations and dumping of the preload ballast would result in additional and unaccounted for loads being applied to the top of the spudcans. This additional load, applied to the foundation soils, will reduce the actual factor of safety below that perceived to be the result of the preload. In order to minimize the risk that slow backflow of soil after preloading will reduce the ability of the foundation soils to withstand anticipated loads during severe storms, it is advisable that the maximum preload ballast be maintained until additional spudcan penetrations under the constant rig load become negligible. Additionally, it is good practice to monitor and plot spudcan load-penetration values throughout the preload operation and to compare with predicted values. Continuous monitoring of spudcan load-penetration values using spreadsheets or more sophisticated programs, such as the program PRELOAD™ by Matthews Daniel Company, are good monitoring tools and can help determine if delayed soil backflow is occurring. Once again, monitoring spudcan penetration while holding the maximum preload until additional penetrations become negligible is the best way to minimize the risk of a loss of the perceived factor of safety at sites where deep spudcan penetrations are expected.

Summary and Recommendations

Spudcan penetration curves were developed using bearing capacity factors recommended by Skempton, Hansen, Houlsby & Martin, and Hossain et al., and are compared to measured spudcan penetration records at thirteen sites in the Gulf of Mexico. A range of jackup rigs were investigated with spudcan equivalent diameters that varied from 10.6 to 19.8 meters and individual spudcan bearing pressures that ranged from 162.8 to 507.4 kPa. The following is a list of the pertinent facts and conclusions from this study.

1. Soil conditions at the sites considered in this study consist of normally to slightly over-consolidated clay profiles with linearly increasing shear strength and submerged unit weight profiles. Soil parameters for these sites are presented in Table 1.

2. Comparisons of predicted and measured spudcan load-penetration curves, shown in Figure 5, indicate that the predicted trends, based on the assumption of complete backflow into the spudcan cavity, generally follow the measured penetration records, but vary between over-predicting, under-predicting and predicting the average of the observed penetrations under a given load.
3. Penetration predictions using Houlsby & Martin bearing capacity factors provide lower bound estimates of the load required to achieve a given spudcan penetration.
4. Penetration predictions using bearing capacity factors recommended by Skempton and Hansen provide good "average" estimates of spudcan penetration under a given load. However, these methods may under-predict or over-predict measured penetrations, depending on soil conditions, spudcan type, and depth of penetration.
5. Penetration predictions based on the Hossain et al., bearing capacity factors provide an upper bound estimate of the load required to achieve a given penetration. Reducing the recommended Hossain et al., bearing capacity values by 20 percent results in predicted penetrations under given loads similar to those obtained with the Skempton and Hansen factors.
6. Measured spudcan penetration records with values supplied for all three legs reveal a scatter in the load-penetration values. Consequently, it is recommended that upper and lower bound load-penetration curves be supplied to the rig operators to best capture the expected range of spudcan load-penetration response.
7. The shape of the spudcan of the Super Gorilla jackup rig has an effect on bearing capacity. An empirical reduction of 15 percent fits the measured penetration data. This reduction is related to the spudcan shape and the low volume of the spudcan tip (cone) relative to the maximum cross-sectional area.
8. The Levingston 111-IC and Marathon LeTourneau 52-S jackup rigs obtain deeper penetrations than the bearing capacity methods predict. An empirical "shape factor" reduction of 10 percent applied to the theoretical bearing capacities results in a better fit to the measured spudcan penetration data. This reduction is likely related to the volume of the spudcan tip (cone) relative to the maximum cross-sectional area.
9. Spudcan cavity depths determined from the Meyerhof stability factor, recommended in SNAME, give cavity depths that would result in theoretical spudcan penetrations under-predicting the observed values. This suggests that the derived soil cavity depths are too deep for the normally to slightly over-consolidated clay profiles in this study.
10. Spudcan cavity depths calculated using the Hossain et al., recommendations provide reasonable results that better fit the assumptions used to determine bearing capacity. Theoretical spudcan cavity depths and observations regarding spudcan cavity stability are shown in Table 3 for the thirteen locations studied.
11. Seven of the spudcan penetration records show additional spudcan penetration occurs while holding maximum preload. The additional penetration is presumed to be the result of unaccounted spudcan load, that is the result of soil backflow into the spudcan cavity, which was assumed to be completely backfilled in the formulations of bearing capacity used in this study.
12. The assumptions of complete backflow into the spudcan cavity in the formulation of the bearing capacity methods yielded reasonable predictions of the load-penetration trends when compared to the measured values. However, these assumptions appear to be contrary to the longer-term load-penetration response at the seven sites where additional penetrations were observed under constant maximum preload, possibly due to soil backflow. Based on this observation, the lower bound predictions of Houlsby & Martin may best predict the final, long term penetrations at locations where full soil backflow occurs while the other methods, particularly the Hansen Method, may yield better predictions at locations where the spudcan cavity stabilizes before full backflow occurs (in spite of the assumption of full backflow).
13. Recommendations resulting from this study are that spudcan penetrations should be continuously monitored during preloading operations and compared to predicted penetration values. At sites where deep penetrations are expected and delayed spudcan cavity instability and soil backflow could result in post-preload reduction in the factor of safety against foundation bearing capacity failure, the maximum preload should be held for a sufficient time until additional spudcan penetrations become negligible.

New studies are recommended to investigate spudcan cavity stability and soil backflow in normally to slightly over-consolidated clays where deep penetrations are expected. Centrifuge and finite modeling incorporating the effects of the leg trusses and cords on temporarily inhibiting soil backflow could be initiated. Field studies could also be performed, possibly using sonar equipment or pressure plates atop the spudcans to estimate spudcan cavity depth and soil backflow during and immediately after the completion of preload activities and before extracting the legs from the soil. These measurements could probably be obtained with little impact on the drilling operations if properly planned.

Acknowledgements
The authors would like to thank the International Association of Drilling Contractors (IADC) for sponsoring a portion of the work presented in this paper. Additional thanks are given to ENSCO Offshore Company, Rowan Companies, GlobalSantaFe Corporation (now Transocean, Inc.), and Diamond Offshore Drilling, Inc., for providing penetration records. Thanks to the Rowan Companies who provided drawings of the Marathon LeTourneau spudcans. Special thanks to Messrs. Bruce Ahrendsen, Han Shi, Ben Lunsford, and Ms. Audrey Wingate of Fugro-McClelland Marine Geosciences, Inc. (FMMG) who

helped with the soil data, analyzing spudcan penetration records, applying spudcan bearing capacity methods, preparing figures and checking final results. Finally, thanks to Messrs. Robert Little and K C Gan for their review of the manuscript.

Nomenclature

γ'_{th} = Computed theoretical submerged unit weight based on water content, kN/m^3
w = Measured water content in percentage
Gs = Specific gravity for Gulf of Mexico clay = 2.75
Q = The ultimate load the soil can support, kN or MN
B = Equivalent diameter (width) of the spudcan, m
L = Equivalent diameter (length) of the spudcan, m
D = Embedment depth of the maximum cross sectional area of the spudcan below the mudline, m
s_{uavg} = Shear strength averaged to some depth beneath the maximum cross section of the spudcan, kPa
γ_H' = Average submerged unit weight of soil from the mudline to the depth of the spudcan cavity, kPa
H = Depth of spudcan cavity from the mudline, m
A = Area of maximum cross section of the spudcan, m^2
γ' = Average submerged unit weight of the soil displaced by the embedded spudcan, kN/m^3
V = The volume of spudcan, m^3
N_{co} = The bearing capacity factor recommended by Houlsby & Martin (2003) or Hossain et al. (2006)
α = The roughness factor for the spudcan soil interface, assumed = 1.0 for this study,
s_{uo} = The shear strength at the depth of maximum cross section area of the spudcan, kPa
β = The angle of the spudcan tip (the larger angle indicated in Figure 2 was used), in degrees
ρ = The rate of increase of the shear strength profile with depth, kPa/m
N_{cd} = The bearing capacity factor for deep spudcan embedment recommended by Hossain et al. (2006)
H_{cr} = The depth at which the spudcan cavity remains stable and constant, m
N = A dimensionless stability factor determined for open excavation by Meyerhof (1972)
γ_o' = The average submerged unit weight of the soil from the mudline to depth H, kN/m^3
S_{uH} = The shear strength at depth, H , (bottom of spudcan cavity), kPa
S_{um} = The shear strength at the mudline, kPa

References

American Petroleum Institute, Gulf of Mexico Jackup Operations for Hurricane Season (Interim Recommendations), API Recommended Practice 95J, 1st Edition, June 2006.

Britto A.M. & Kusakabe, Osanu, 1983, Stability of Axisymmetric Excavations in Clays, Journal of Geotechnical Engineering, Vol. 109, No. 5, 666-681.

Gemeinhardt, J.P. & Focht, J.A., 1970, Theoretical and Observed Performance of Mobile Rig Footings on Clay, Proceedings Offshore Technology Conference, Houston, OTC 1201.

Hansen, J.B., 1970, A Revised and Extended Formula for Bearing Capacity, Bulletin No. 28, Danish Geotechnical Institute, Copenhagen, pp. 5-11.

Houlsby, G.T. & Martin, C.M., 2003, Undrained Bearing Capacity Factors for Conical Footings on Clay, Geotechnique, 53(5), 513-520.

Hossain, M.S., Randolph, M.F., Hu, Y., & White, D.J., 2006, Cavity Stability and Bearing Capacity of Spudcan Foundations on Clay, Offshore Technology Conference, Houston, OTC 17770,

InSafeJIP, 2009, A Joint Industry Project in Progress.

ISO, Petroleum and Natural Gas Industries – Offshore Structures, Part 4, Geotechnical and Foundation Design Consideration, International Organization for Standardization, 2003, ISO 19901-4.

Jack, R.L., Hoyle, M.J.R., Hunt, R.J., & Smith, N.P., 2007, Jack-Up Accident Statistics: Lots to Learn!, Proceeding of the 11th International Conference, The Jackup-Platform, Design, Construction & Operation, Sept. 11 & 12th, London, England.

Meyerhof, G.G., 1972, Stability of Slurry Trench Cuts in Saturated Clay, Proceeding Specialty Conference Performance of Earth and Earth Supported Structures, 1, 1451-1166.

Morandi, A.C., 2007, Jackup Operations in the Gulf of Mexico, Lessons Learned from Recent Hurricanes, Proceeding of the 11th International Conference, The Jackup-Platform, Design, Construction & Operation, Sept. 11 & 12th, London, England.

Quiros, G.W., Young, A.G, Pelletier, J.H., and Chan, J.H-C., 1983, Shear Strength Interpretation for Gulf of Mexico Clays, Proceedings of the Conference on Geotechnical Practice in Offshore Engineering, Austin, April, 144-165.

Quiros, G.W., Aramburu, J.G., & Peters, P. M., 2008, Comparison of Axial Capacities in Clay at Offshore Sites Investigated by Both Early and Recent Sampling Techniques, *Proceedings, 40th Annual Offshore Technology Conference*, Houston, OTC Paper 19569.

Skempton, A.W., 1951, The Bearing Capacity of Clays, Building Research Congress, London 1, 180-189.
Society of Naval Architects of Marine Engineers - SNAME, Guidelines for Site Specific Assessment of Mobile Jack-Up Units, SNAME T&R Bulletin 5-5A, Jersey City, New Jersey, 1st Edition –Rev 2, January, 2002.
Young, A.G., Remmes, B.D., & Meyer, B.J., 1984, Foundation Performance of Offshore Jack-up Drilling Rigs, Journal of Geotechnical Engineering, ASCE, 110(7), 841-859.

Tables

Table 1 Soil Properties for Thirteen Gulf of Mexico Sites

Site Designation	Number of Soil Layers	Penetration m	Shear Strength kPa	Shear Strength Rate Increase kPa/m	Submerged Unit Weight KN/m³	Comments
1	1	0	2.4	1.35	4.7	Normally Consolidated
		42.7	59.9		6.8	
2	1	0	2.4	1.59	4.7	Normally Consolidated
		48.2	79		7.7	
3	1	0	2.4	1.43	4.7	Normally Consolidated
		43.6	64.7		6.8	
4	1	0	19.2	1.46	6	Slightly Over-Consolidated
		25.9	57		6.4	
5	1	0	15.6	1.24	5.7	Slightly Over-Consolidated
		24.1	45.5		6.6	
6	2	0	4.8	1.19	4.4	Normally Consolidated
		10.1	16.8		4.9	
		10.1	26.31	2.01	6.8	Slightly Over-Consolidated
		45.7	98.2		6.9	
7	1	0	5.7	1.18	5.5	Normally Consolidated
		45.7	59.9		6.8	
8	1	0	8.6	1.02	4.9	Slightly Over-Consolidated
		30.5	39.8		6.3	
9	1	0	23	1.26	6.6	Slightly Over-Consolidated
		18.3	46		6.6	
10	2	0	12.5	1.37	5.7	Slightly Over-Consolidated
		2.4	15.8		5.7	
		2.4	21.6	1.63	5.7	Slightly Over-Consolidated
		45.1	91		7.2	
11	1	0	9.6	1.62	5.5	Slightly Over-Consolidated
		19.2	40.7		6.1	
12	1	0	18.2	2.09	5.8	Slightly Over-Consolidated
		13.4	46.2		5.8	
13	1	0	18.2	1.2	6.6	Slightly Over-Consolidated
		24.7	47.9		6.6	

Table 2 Jackup Rig Spudcan Loads and Dimensions

SITE	JACKUP RIG TYPE	EQUVILENT DIAMETER (m)	MAXIMUM BEARING AREA (m^2)	SPUDCAN VOLUME (m^3)	MAXIMUM BEARING PRESSURE (kPa)
1	MLT 116-C (Super 116-C)	13.5	143.6	275.0	478.7
2	MLT 116-C (Enhanced 116-C)	13.5	143.6	275.0	402.1
3	MLT 84 (Enhanced 84)	13.7	147.2	318.0	392.5
4	MLT 82-SDC	12.0	113.8	254.8	325.5
5	MLT 82-SDC	12.0	113.8	254.8	311.2
6 &10	MLT 224-C (Super Gorilla)	19.8	306.7	1,327.0	507.4
7,8,9	MLT 82-SDC	12.0	113.8	254.8	282.4
11	MLT 150-44-C	10.6	87.7	215.2	253.7
12	LEV-111-IC	14.6	168.1	380.8	277.6
13	MLT 52-S	14.2	158.0	257.7	162.8

Table 3 Spudcan Penetration and Cavity Depths

Site Designation	(1) D (m)	(2) D/B	Depth of Spudcan Cavity (m)		(3) Observed Cavity Behavior	Comments
			SNAME Method	Hossain et al. Method		
1	37.5	2.8	8.5	3.4	Unstable	One Soil Layer
2	24.5	1.8	> 24.5	3.7	Stable	One Soil Layer
3	30.0	2.2	12.0	3.4	Stable	One Soil Layer
4	14.2	1.2	14.2	5.8	Unstable	One Soil Layer
5	17.3	1.4	> 17.3	5.5	Unstable	One Soil Layer
6	32.4	1.6	12.4	5.8	-	Two Soil Layers
7	22.3	1.9	14.5	3.7	Unstable	One Soil Layer
8	23.6	2.0	> 23.6	4.2	Unstable	One Soil Layer
9	8.4	0.7	> 8.4	6.1	Unstable	One Soil Layer
10	34.5	1.7	5.8	7.9	-	Two Soil Layers
11	11.4	1.1	> 11.4	4.6	-	One Soil Layer
12	10.3	0.7	> 10.3	7.3	Unstable	One Soil Layer
13	4.4	0.3	> 4.4	5.5	-	One Soil Layer

(1) Maximum depth from mudline to maximum cross-sectional area of spudcan.

(2) Ratio of maximum spudcan depth to diameter.

(3) Soil backflow stability observed from spudcan penetration records.

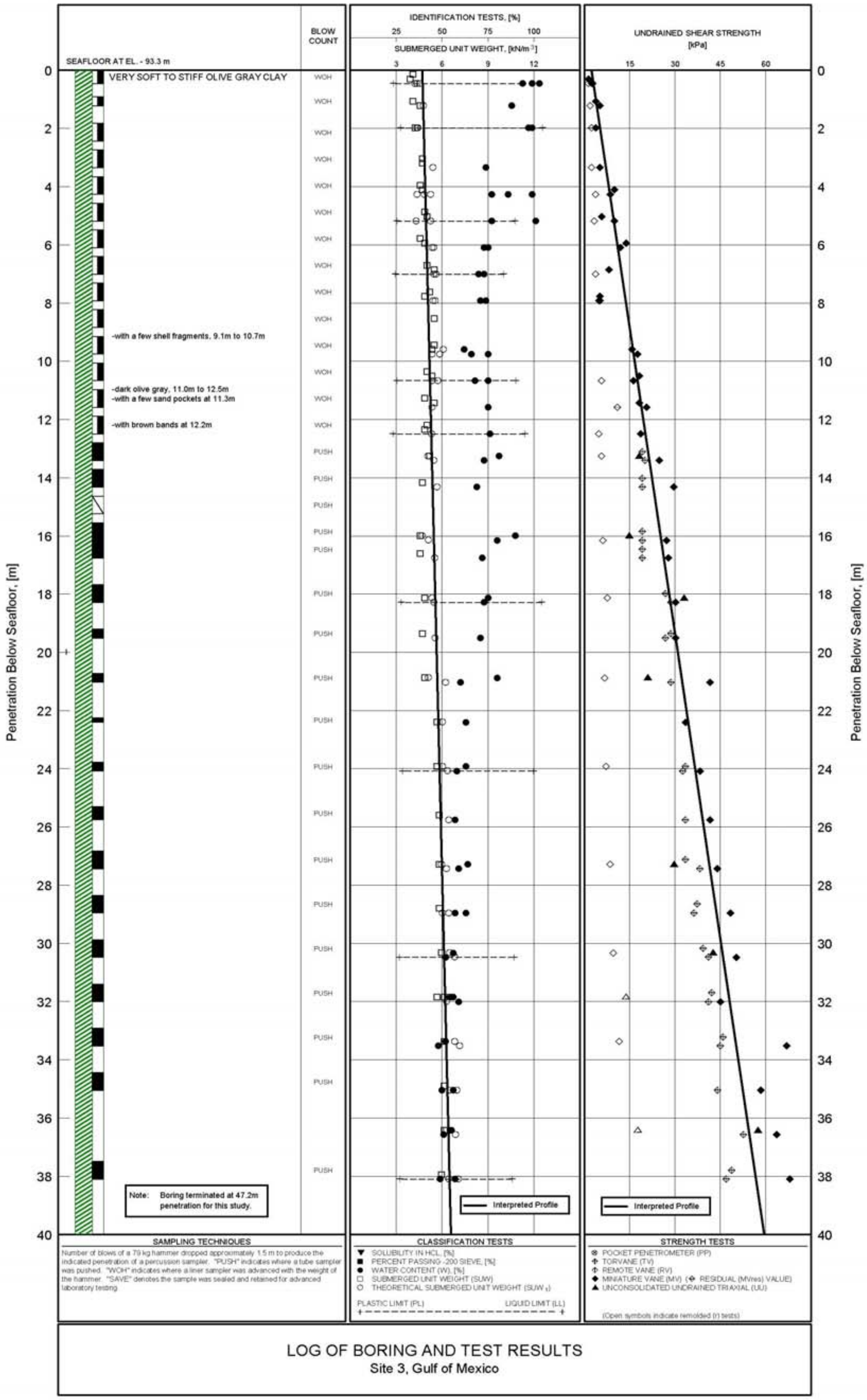

Fig. 1a Normally Consolidated Soil Profile for Site 3

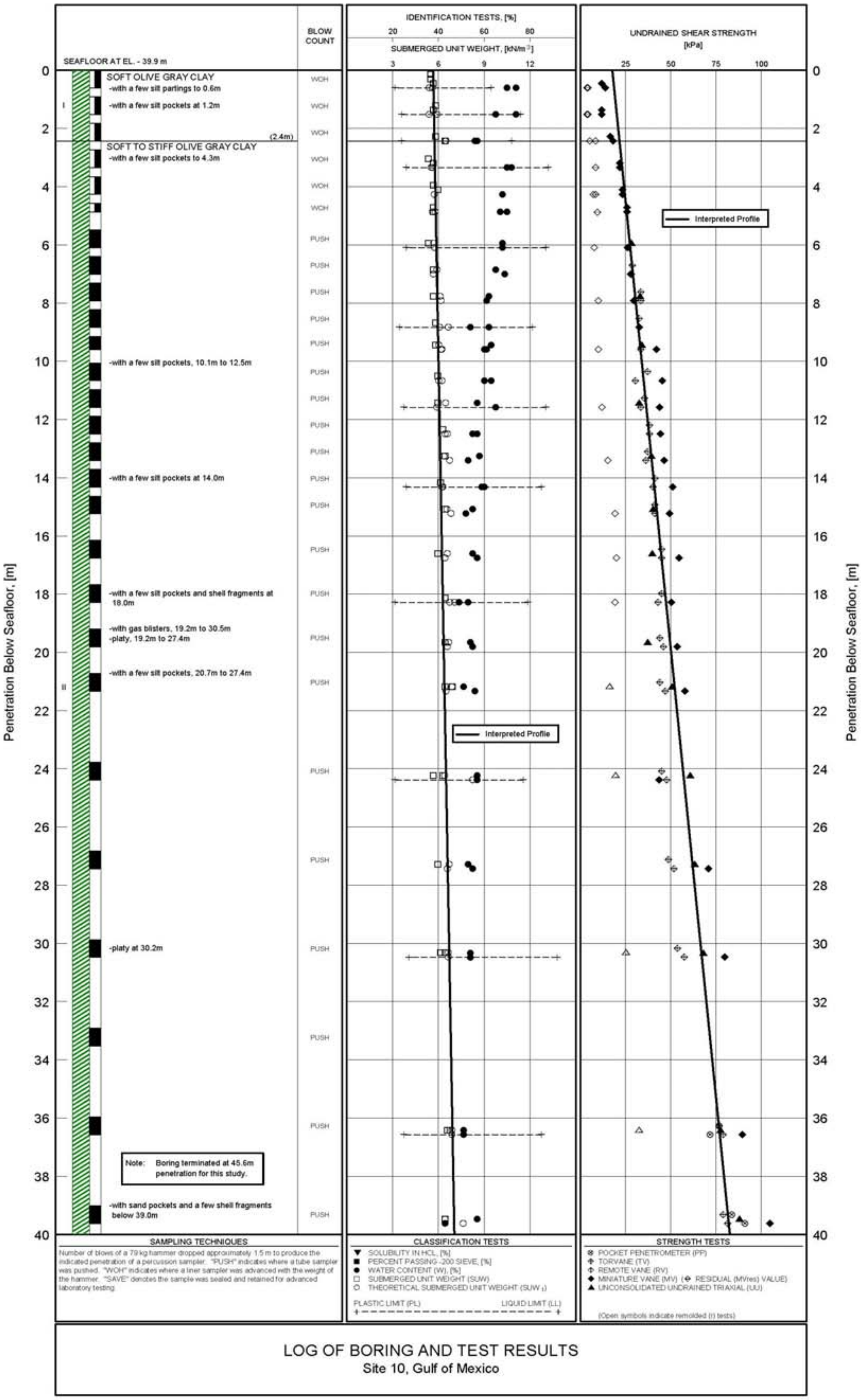

Fig. 1b Slightly Over-Consolidated Soil Profile for Site 10

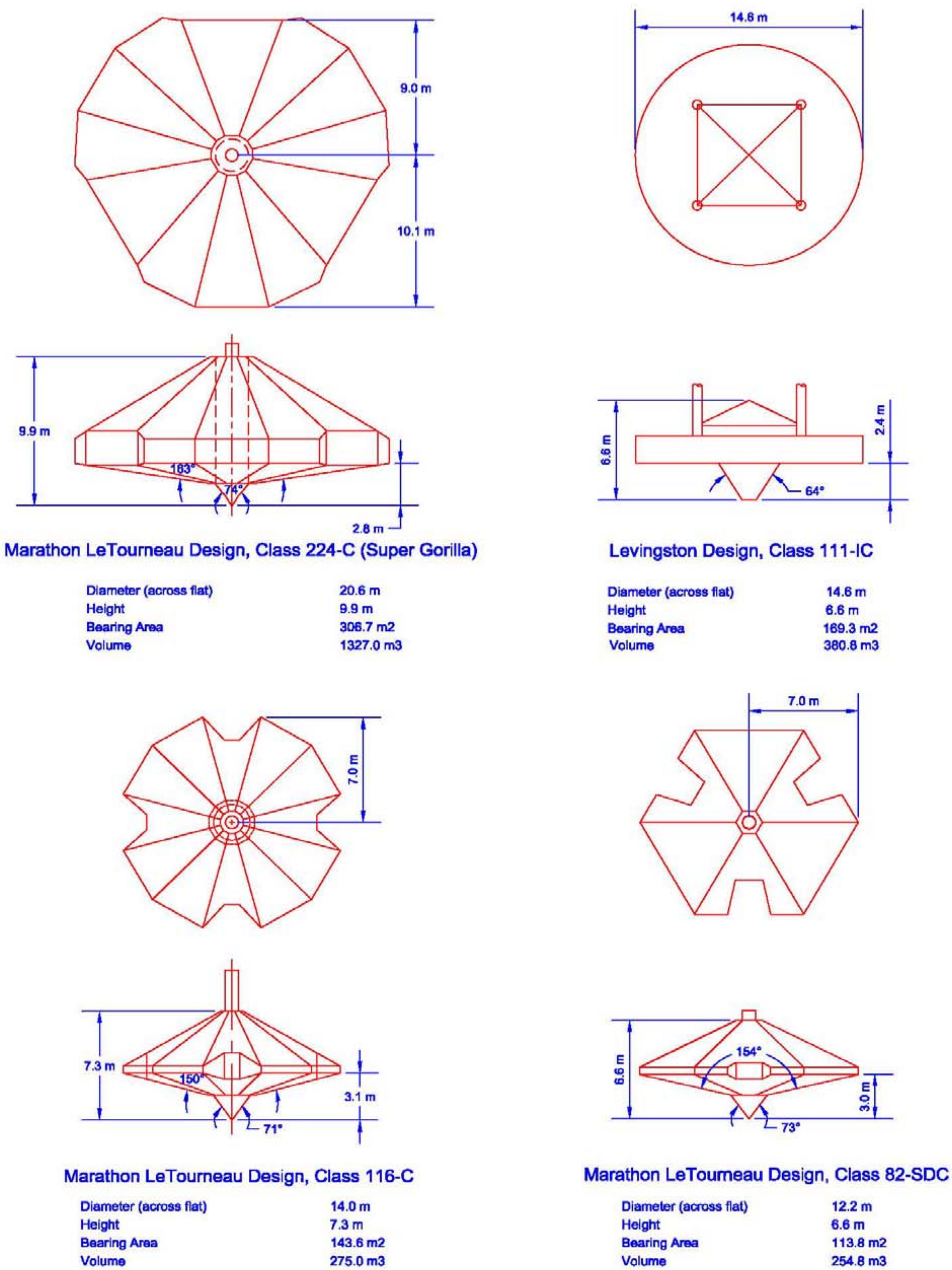

Fig. 2 Spudcan Geometry and Dimensions

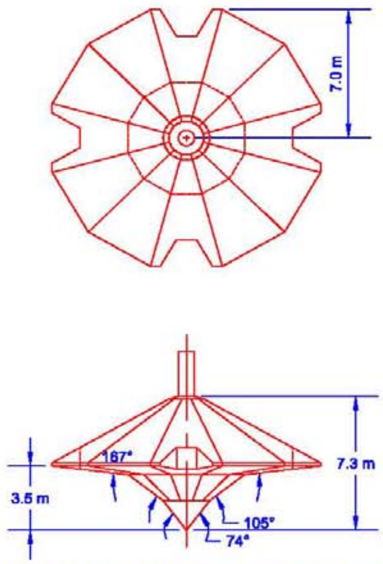

Marathon LeTourneau Design, Class 84

Diameter (across flat)	14.0 m
Height	7.3 m
Bearing Area	147.2 m2
Volume	318.0 m3

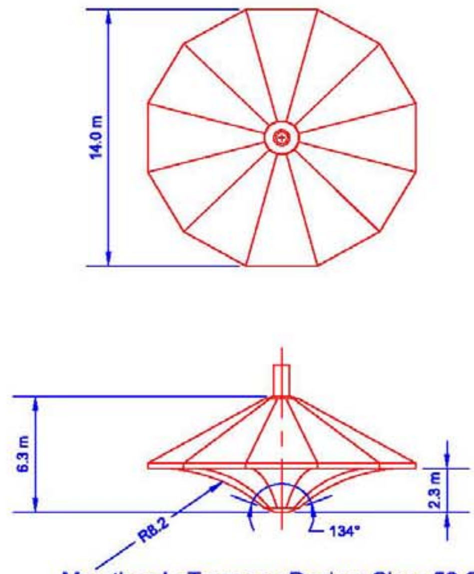

Marathon LeTourneau Design, Class 52-S

Diameter (across flat)	14.0 m
Height	6.3 m
Bearing Area	158.0 m2
Volume	257.7 m3

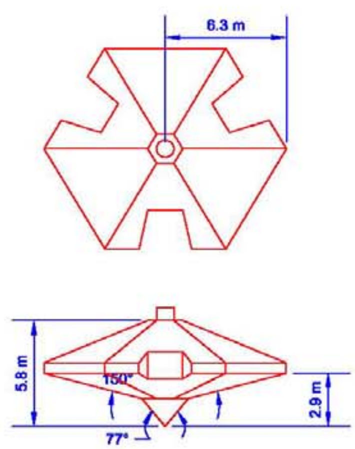

Marathon LeTourneau Design, Class 150-44-C

Diameter (across flat)	11.0 m
Height	5.8 m
Bearing Area	87.7 m2
Volume	215.2 m3

Fig. 2 (Cont.) Spudcan Geometries and Dimensions

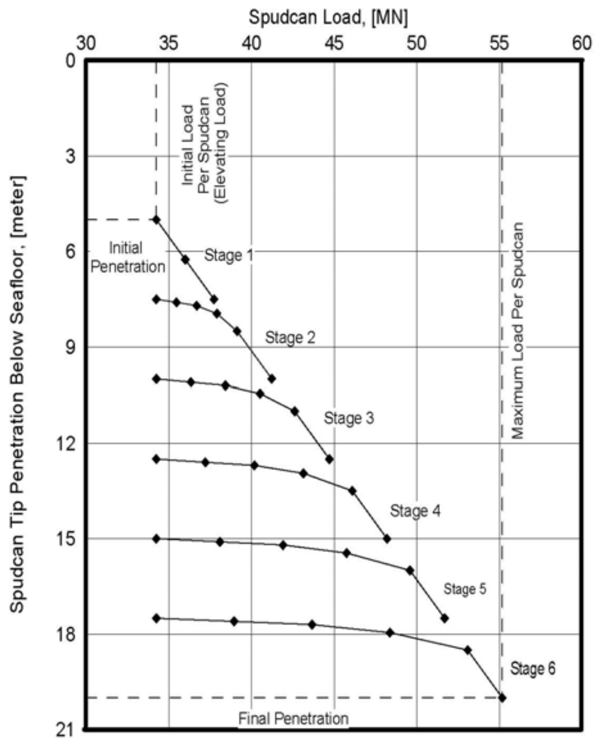

Fig. 3a Idealized Spudcan Penetration Record

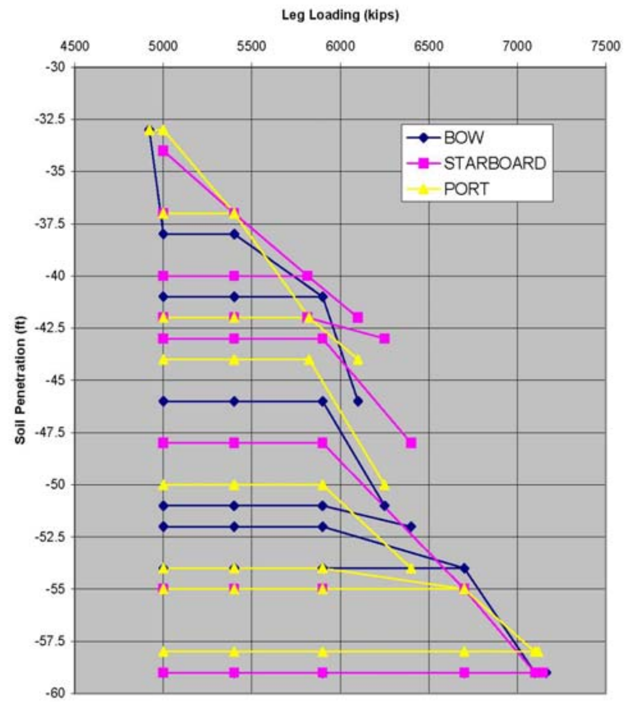

Fig. 3b Measured Spudcan Penetration Record

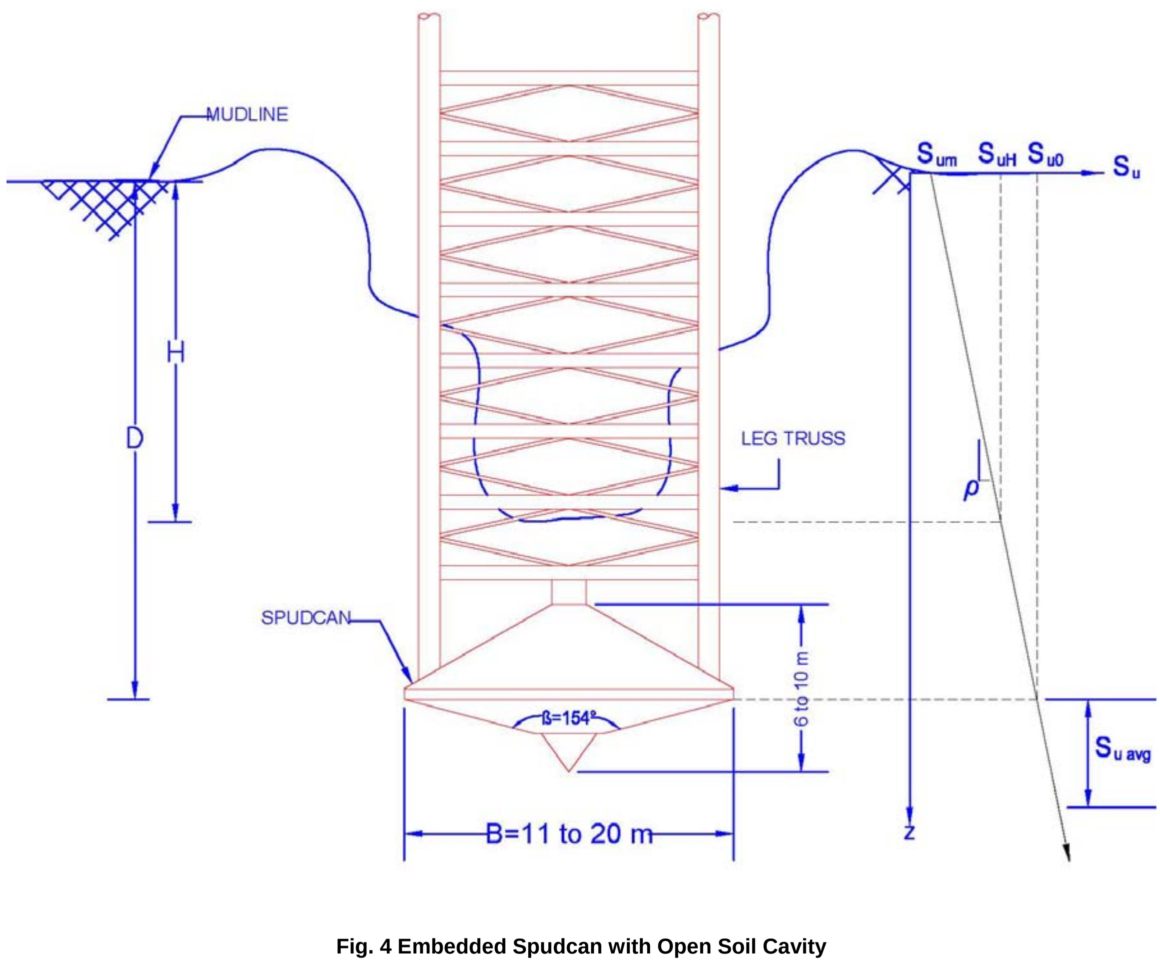

Fig. 4 Embedded Spudcan with Open Soil Cavity

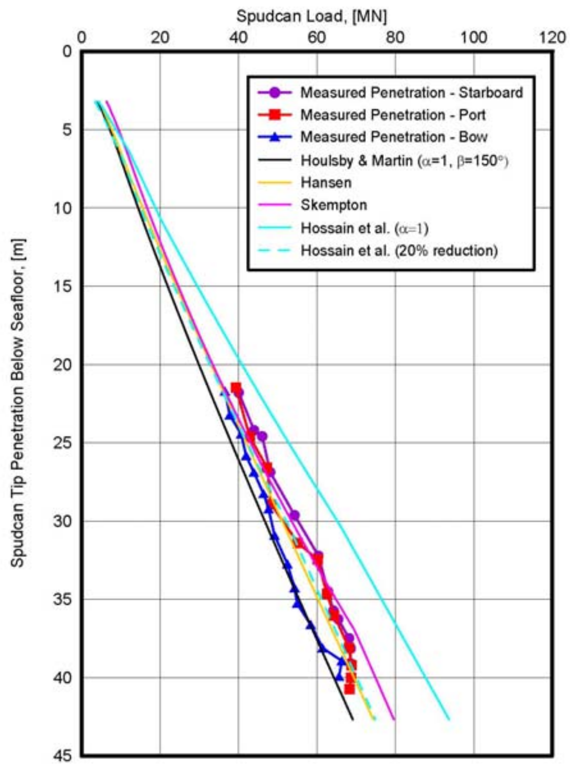

SPUDCAN PENETRATION CURVE
Marathon LeTourneau Design, Class 116-C
Site 1, Gulf of Mexico

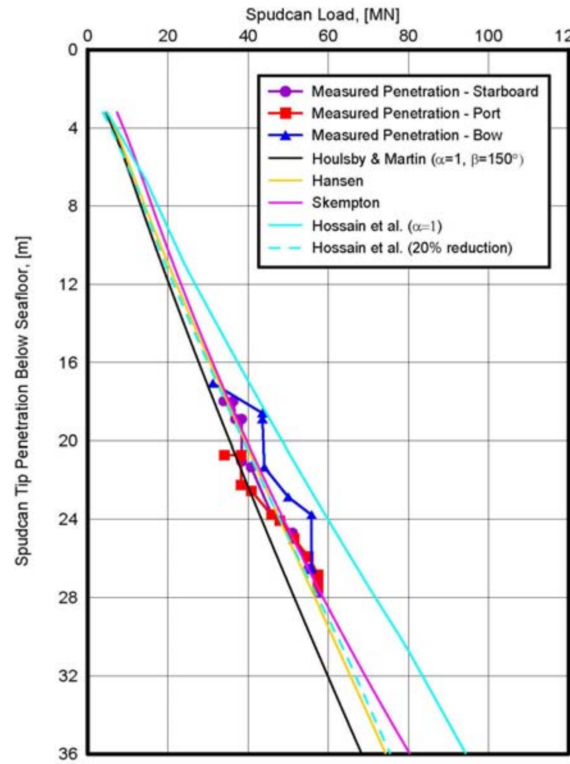

SPUDCAN PENETRATION CURVE
Marathon LeTourneau Design, Super Class 116-C
Site 2, Gulf of Mexico

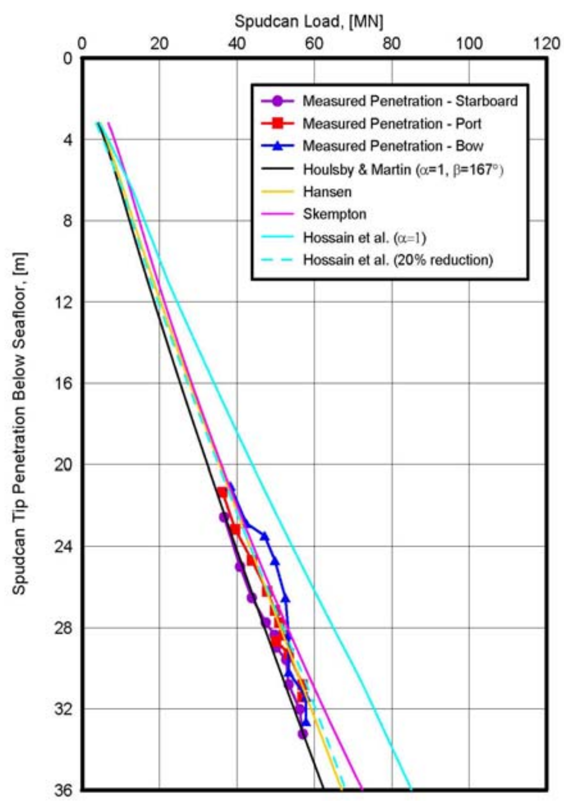

SPUDCAN PENETRATION CURVE
Marathon LeTourneau Design, Class 84
Site 3, Gulf of Mexico

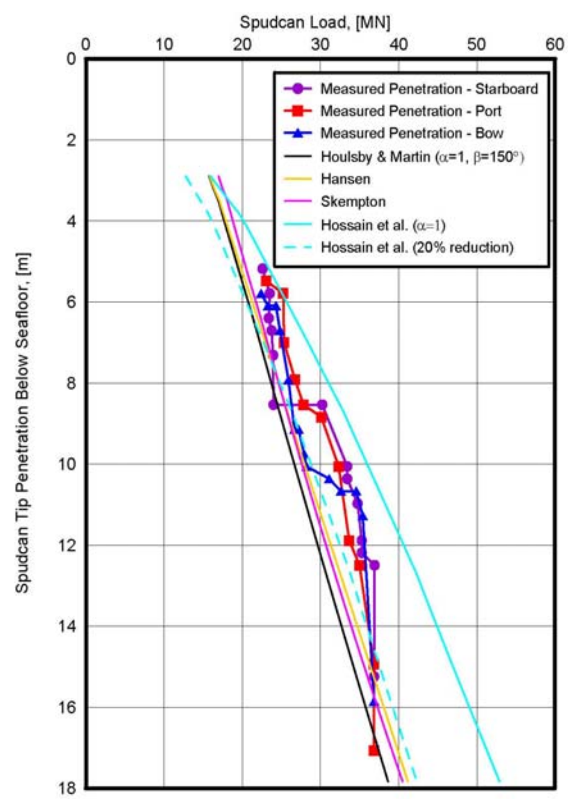

SPUDCAN PENETRATION CURVE
Marathon LeTourneau Design, Class 82-SDC
Site 4, Gulf of Mexico

Fig. 5 Comparison of Bearing Capacity Methods

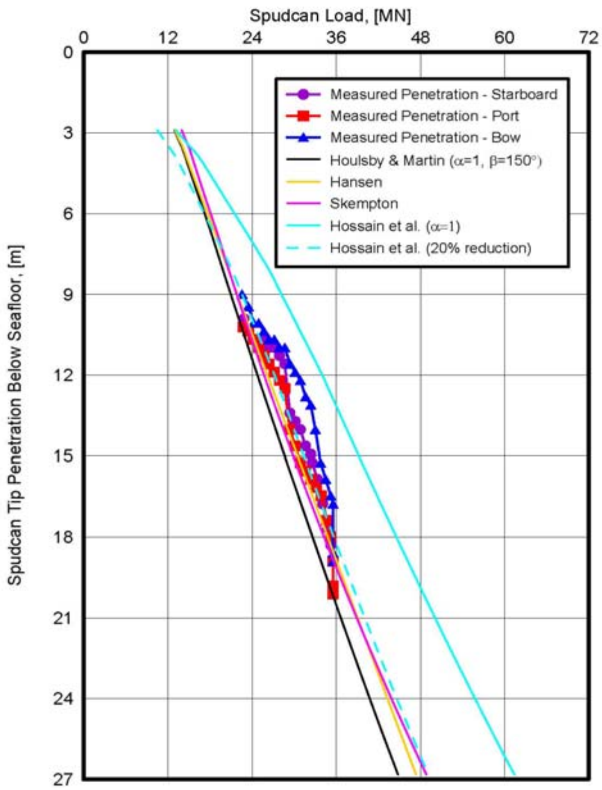

SPUDCAN PENETRATION CURVE
Marathon LeTourneau Design, Class 82-SDC
Site 5, Gulf of Mexico

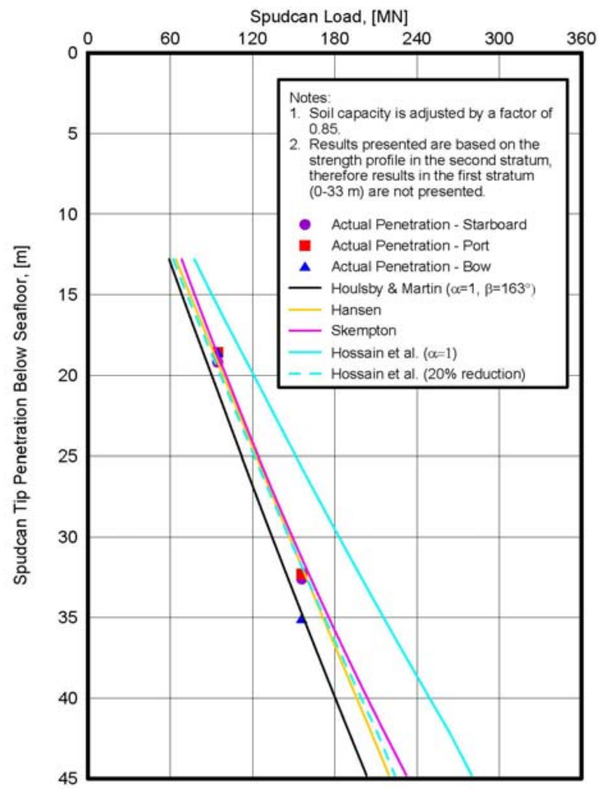

SPUDCAN PENETRATION CURVE
Marathon LeTourneau Design, Enhanced Gorilla Class
Site 6, Gulf of Mexico

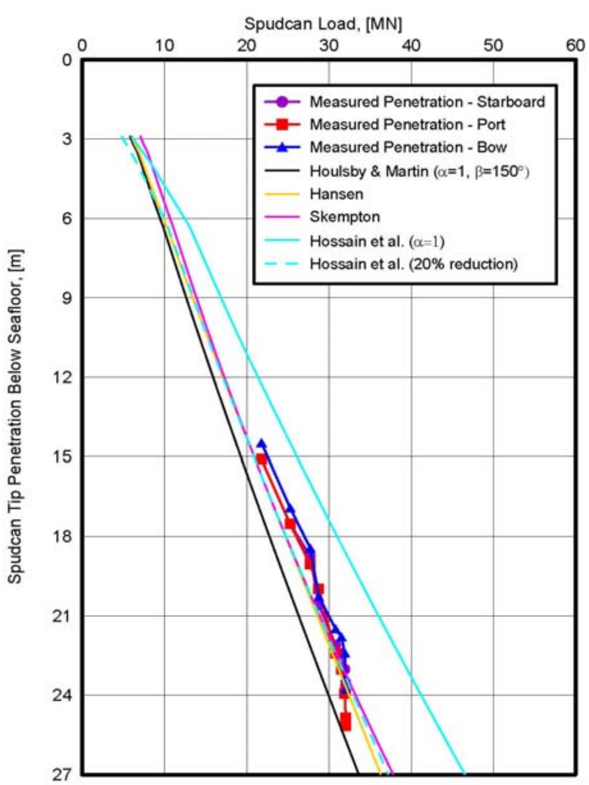

SPUDCAN PENETRATION CURVE
Marathon LeTourneau Design, Class 82-SDC
Site 7, Gulf of Mexico

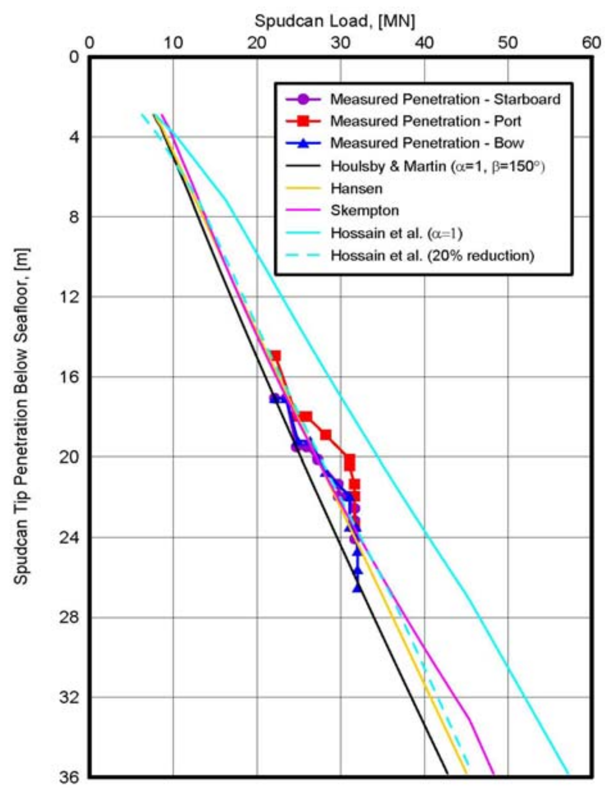

SPUDCAN PENETRATION CURVE
Marathon LeTourneau Design, Class 82-SDC
Site 8, Gulf of Mexico

Fig. 5 (Cont.) Comparison of Bearing Capacity Methods

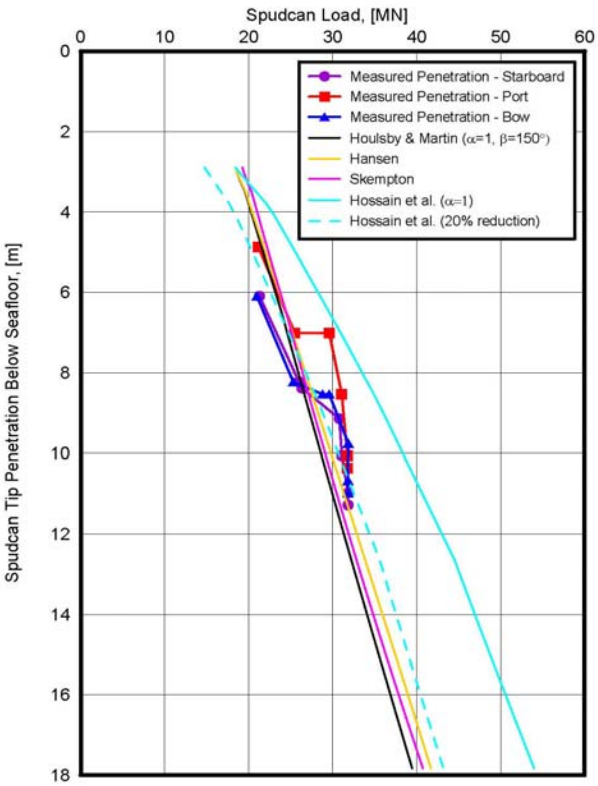

SPUDCAN PENETRATION CURVE
Marathon LeTourneau Design, Class 82-SDC
Site 9, Gulf of Mexico

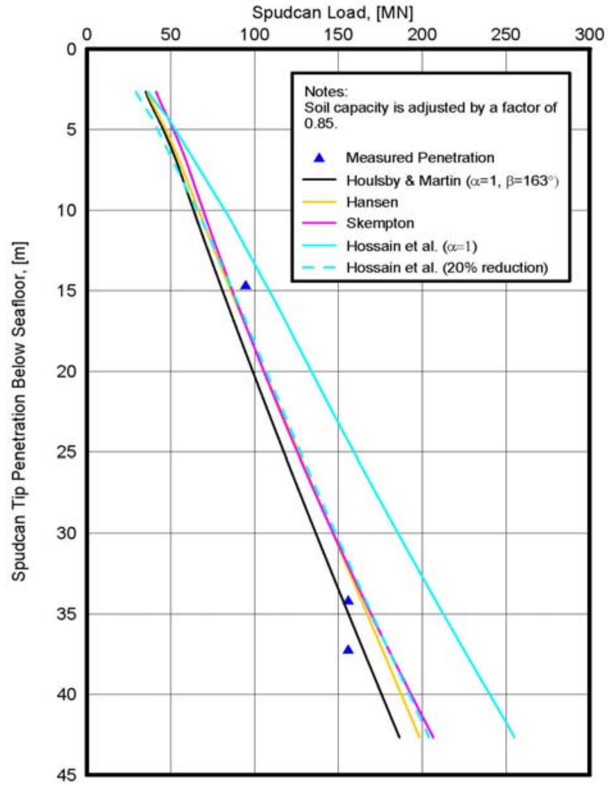

SPUDCAN PENETRATION CURVE
Marathon LeTourneau Design, Enhanced Gorilla Class
Site 10, Gulf of Mexico

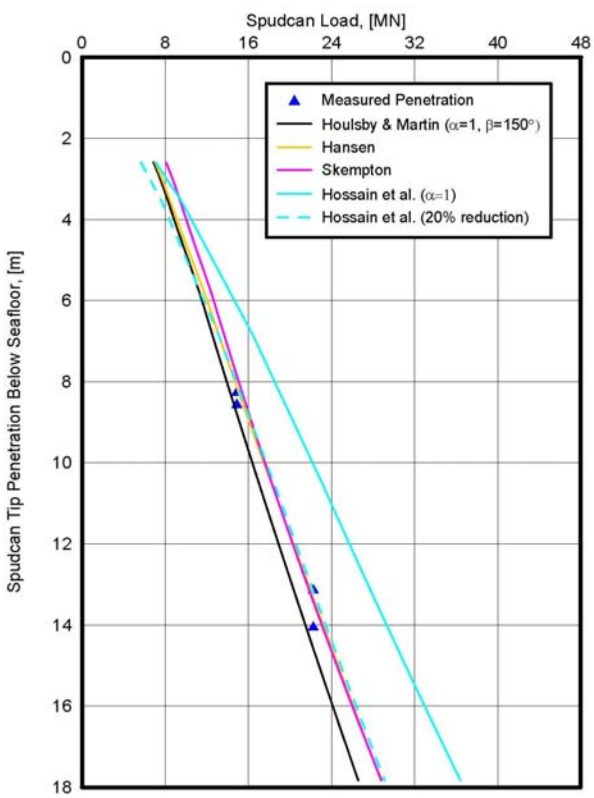

SPUDCAN PENETRATION CURVE
Marathon LeTourneau Design, Class 150-44-C
Site 11, Gulf of Mexico

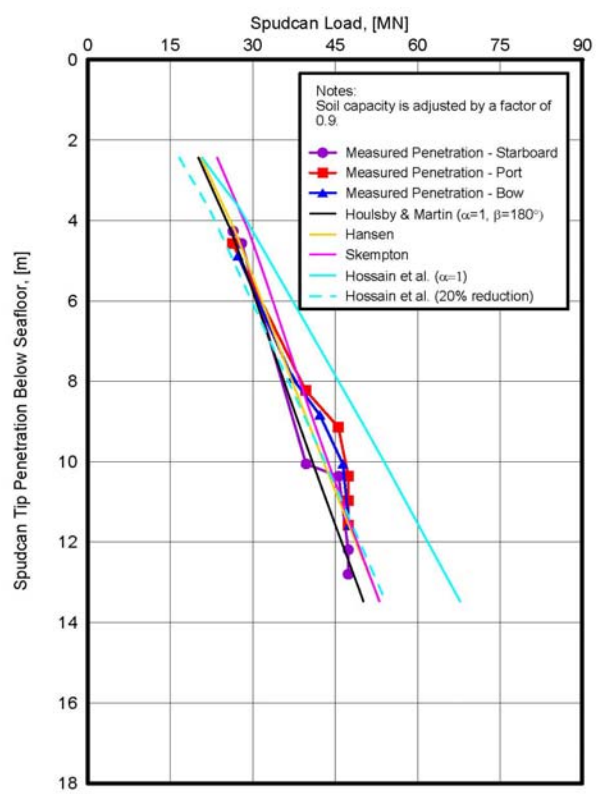

SPUDCAN PENETRATION CURVE
Levingston 111-IC
Site 12, Gulf of Mexico

Fig. 5 (Cont.) Comparison of Bearing Capacity Methods

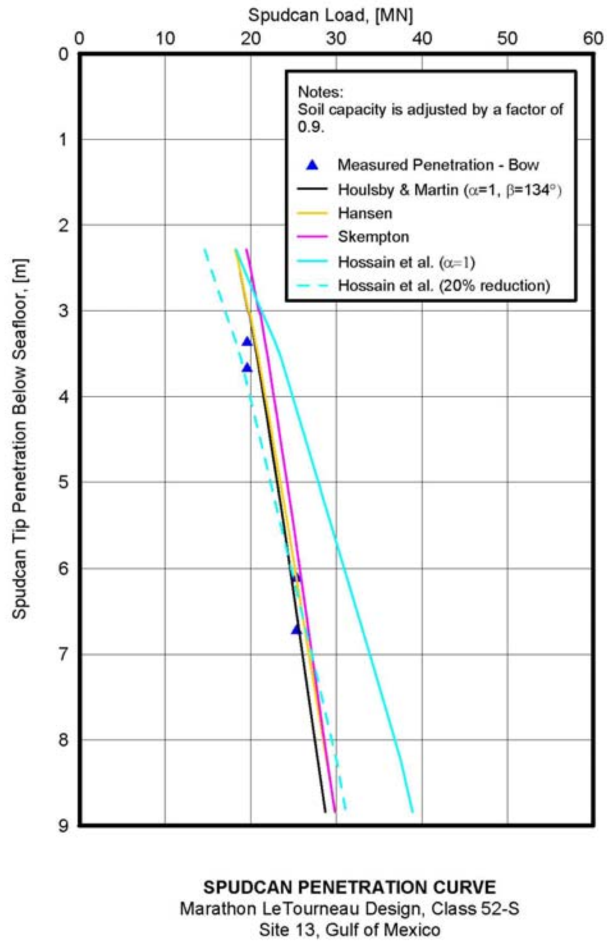

Fig. 5 (Cont.) Comparison of Bearing Capacity Methods